Available online at www.sciencedirect.com

ScienceDirect

Nuclear Physics B 909 (2016) 1079–1103

NUCLEAR PHYSICS B

www.elsevier.com/locate/nuclphysb

Checking T and CPT violation with sterile neutrino

Yogita Pant, Sujata Diwakar, Jyotsna Singh *, R.B Singh

Department of Physics, University of Lucknow, Lucknow 226007 India

Received 16 February 2016; received in revised form 13 May 2016; accepted 23 May 2016

Available online 1 June 2016

Editor: Tommy Ohlsson

Abstract

Post LSND results, sterile neutrinos have drawn attention and motivated the high energy physics, astronomy and cosmology to probe physics beyond the standard model considering minimal $3+1$ (3 active and 1 sterile) to $3+N$ neutrino schemes. The analytical equations for neutrino conversion probabilities are developed in this work for $3+1$ neutrino scheme. Here, we have tried to explore the possible signals of T and CPT violations with four flavor neutrino scheme at neutrino factory. Values of sterile parameters considered in this analysis are taken from two different types of neutrino experiments viz. long baseline experiments and reactor+atmospheric experiments. In this work golden and discovery channels are selected for the investigation of T violation. While observing T violation we stipulate that neutrino factory working at 50 GeV energy has the potential to observe the signatures of T violation through discovery channel if sterile parameter values are equal to that taken from reactor+atmospheric experiments. The ability of neutrino factory for constraining CPT violation is enhanced with increase in energy for normal neutrino mass hierarchy (NH). Neutrino factory with the exposure time of 500 kt-yr will be able to capture CPT violation with $\delta c_{31} \geq 3.6 \times 10^{-23}$ GeV at 3σ level for NH and for IH with $\delta c_{31} \geq 4 \times 10^{-23}$ GeV at 3σ level.

1. Introduction

The standard model of particle physics considers neutrinos to be massless. Sudbury Neutrino Observatory [1,2] gave evidence of neutrino oscillations which was further confirmed by Kam-

* Corresponding author.
E-mail address: singh_jyotsna@lkouniv.ac.in (J. Singh).

http://dx.doi.org/10.1016/j.nuclphysb.2016.05.021

LAND experiment [3]. This landmark research assigned mass to the neutrinos and gave a clear indication of new physics beyond the standard model. A simple stretch in the standard model was able to stand up with the mass of neutrino. In neutrino physics the standard three flavor neutrino oscillations can be explained with the help of six parameters namely θ_{12}, θ_{13}, θ_{23}, Δm^2_{12}, Δm^2_{31} and δ_{CP}. Amongst these six parameters, solar parameters (θ_{12}, Δm^2_{12}) and atmospheric parameters (θ_{23}, Δm^2_{31}) have been measured with high precision. Furthermore, Daya Bay and RENO reactor experiments have strongly constrained the value of mixing angle θ_{13}. Now we are in need of such neutrino experiments which can impose tight constraints on the value of δ_{CP} and mass hierarchy. Some anomalies popped up while observing appearance channel and disappearance channel of ν_e at LSND experiment. While observing $\bar{\nu}_\mu \to \bar{\nu_e}$ appearance channel, LSND [4–9] was the first experiment to publish evidence of a signal at $\Delta m^2 \sim 1$ eV^2. Later in 2002, MiniBooNE [10,11] checked the LSND result for $\nu_e \to \nu_\mu$ ($\bar{\nu}_e \to \bar{\nu}_\mu$) appearance channel. At MiniBooNE experiment, while observing the CCQE events rate through $\nu_e n \to e^- p (\bar{\nu}_e p \to e^+ n)$ above 475 MeV energy, no excess events were found but for energies < 475 MeV $\nu_e(\bar{\nu}_e)$ excess events were observed. In this way, MiniBooNE data supported the LSND result. The LEP data [12,13] advocates the number of weakly interacting light neutrinos, that couple with the Z bosons through electroweak interactions, to be 2.984 ± 0.008; thus closing the door for more than three active neutrinos. Hence, the heavy neutrino announced by LSND group should be different from these three active neutrinos. This higher mass splitting in the standard three active neutrino model was accommodated by introducing sterile neutrinos. Sterile neutrinos carry a new flavor which can mix up with the other three flavors of standard model but they do not couple with W and Z bosons. The number of sterile neutrinos can vary from minimum one to any integer N.

Some cosmological evidences like CMB anisotropies [14–18] and Big Bang nucleosynthesis [19,20] also stood up with the LSND data. The results reported by the combined analysis [21] of Baryonic Acoustic Oscillations (BAO) [22–26] 'H_0 + PlaSZ + Shear + RSD' indicated the presence of sterile neutrinos, by stipulating the number of effective neutrinos $N_{eff} \equiv 3.62^{+0.26}_{-0.42}$, $m_\nu^{eff}(sterile) = 4.48^{+0.11}_{-0.14}$ eV and giving preference for $\triangle N_{eff} \equiv N_{eff} - 3.62^{+0.26}_{-0.42}$ at 1.4σ level and non-zero mass of sterile neutrino at 3.4σ level. The gallium solar neutrino experiments (gallium anomaly) GALLEX [27], SAGE [28] and the antineutrino reactor experiments ($\bar{\nu}_e$) like Bugey-3, Bugey-4, Gosgen, Kransnogark, IIL [29] (reactor anomaly) indicated that electron neutrinos and antineutrinos may disappear at short baselines. Such disappearance can be explained by the presence of at least one massive neutrino (of the order of 1 eV). Thus, these experiments also indicated the presence of sterile neutrino and supported the LSND results. Some constraints imposed by the combined fit of reactor, gallium, solar and $\nu_e C$ scattering data are $\triangle m^2_{41} \gtrsim 1$ eV^2 and $0.07 \leq \sin^2 2\nu_{ee} \lesssim 0.09$ at 95% CL [30]. Few atmospheric neutrino experiments such as IceCube [31], MINOS [32–34], CCFR [35] have also imposed strong constraints on sterile parameters.

The four flavors of neutrino can be studied in either of the two different neutrino mass schemes, 3 + 1 or 2 + 2 schemes [36]. For our work we have selected (3 + 1) four flavor neutrino mass scheme. In this framework, Maki–Nakagawa–Sakata (MNS) mixing matrix (4×4), includes six mixing angles θ_{ij}, three Dirac phases and three Majorana phases.

Neutrino factory [37,38] provides excellent sensitivity to the standard neutrino oscillation parameters and therefore seems to be one of the promising option to explore and reanalyze the global fits for sterile neutrino parameters. To mention, it provides a platform to constrain one of the most searched CP violation in leptonic sector [39,40]. Hence neutrino factory seems to provide a promising environment for the study of T and CPT violation. The neutrino factory set

up considered here is based on the International Design Study of Neutrino Factory [IDS-NF] [41, 42]. As we know that in long baseline neutrino experiments matter effects are significant and CP asymmetric earth matter gives non zero magnitude to ΔP_{CP} even in the absence of CP phase. Therefore, instead of checking ΔP_{CP}, variation in ΔP_T can be studied to probe the extent of true CP violation. We have observed T violation through $\nu_\mu \to \nu_e$ golden channel and $\nu_\mu \to \nu_\tau$ discovery channel and CPT violation along $\nu_\mu \to \nu_\mu$ disappearance channel.

Our work is organized as follows. In section 2, we illustrate $3+1$ neutrino matrix parametrization. In next section, T violating effects are checked for different channels. In section 4, bounds on CPT violating terms are checked in presence of sterile neutrino. In the last section, we have summarized our study and discussed the results observed.

2. Standard parametrization in 3 + 1 neutrino scheme

To check T and CPT violation we have selected $3+1$ neutrino scheme for our analysis. In this scheme the flavor eigenstates ν_α ($\alpha = e, \mu, \tau, s$) and mass eigenstates ν_j ($j = 1, 2, 3, 4$) are related by the given unitary transformation equation[1]

$$\begin{pmatrix} \nu_e \\ \nu_\mu \\ \nu_\tau \\ \nu_s \end{pmatrix} = U \begin{pmatrix} \nu_1 \\ \nu_2 \\ \nu_3 \\ \nu_4 \end{pmatrix} \tag{1}$$

Here unitary matrix (U) can be parametrized in terms of six mixing angles ($\theta_{12}, \theta_{13}, \theta_{23}, \theta_{14}, \theta_{24}, \theta_{34}$), three Dirac phases δ_l ($\delta_1, \delta_2, \delta_3$) and three Majorana phases. Majorana phases are neglected in our study as they do not affect the neutrino oscillations in any realistically observable way. In principle, there are different parametrization schemes for the neutrino mixing matrix as their order of sub-rotation is arbitrary. Our selection for parametrization of neutrino mixing matrix is

$$U = U_{34}(\theta_{34}, 0)U_{24}(\theta_{24}, 0)U_{14}(\theta_{14}, 0)U_{23}(\theta_{23}, \delta_3)U_{13}(\theta_{13}, \delta_2)U_{12}(\theta_{12}, \delta_1) \tag{2}$$

where $U_{ij}(\theta_{ij}, \delta_l)$, the complex rotation matrix in the ij plane can be defined as

$$[U_{ij}(\theta_{ij}, \delta_l)]_{pq} = \begin{cases} \cos\theta_{ij} & p = q = i, j \\ 1 & p = q \neq i, j \\ \sin\theta_{ij} e^{-i\delta_l} & p = i,\ q = j \\ -\sin\theta_{ij} e^{i\delta_l} & p = j,\ q = i \\ 0 & \text{otherwise} \end{cases} \tag{3}$$

Since matrices 14 and 23 commute therefore the order of rotation between them is arbitrary. When neutrinos pass through the earth matter, the charge current interactions (CC) of ν_e and neutral current interactions (NC) of ν_e, ν_μ, ν_τ with the matter give rise to a CC and NC potentials V_e and V_n respectively. While studying the sterile neutrinos, potential V_n can not be neglected. The effective CPT violating hamiltonian (H_f) of neutrinos can be expressed as

[1] A N × N unitary matrix contains N(N − 1)/2 mixing angles and (N − 1)(N − 2)/2 Dirac type CP violating phases. It will also contain (N − 1) number of additional Majorana Phases if the neutrinos are considered as Majorana particles.

$$H_f = \frac{1}{2E}[U \begin{pmatrix} 0 & 0 & 0 & 0 \\ 0 & \Delta m^2_{21} & 0 & 0 \\ 0 & 0 & \Delta m^2_{31} & 0 \\ 0 & 0 & 0 & \Delta m^2_{41} \end{pmatrix} U^\dagger + U_b \begin{pmatrix} 0 & 0 & 0 & 0 \\ 0 & \delta c_{21}.2E & 0 & 0 \\ 0 & 0 & \delta c_{31}.2E & 0 \\ 0 & 0 & 0 & \delta c_{41}.2E \end{pmatrix} U_b^\dagger + \begin{pmatrix} A_e + A_n & 0 & 0 & 0 \\ 0 & A_n & 0 & 0 \\ 0 & 0 & A_n & 0 \\ 0 & 0 & 0 & 0 \end{pmatrix}] \tag{4}$$

Here $A_{e(n)} = 2EV_{e(n)}$, $V_e = \sqrt{2}G_F N_e$ and $V_n = -G_F N_n/\sqrt{2}$. G_F is the Fermi constant, N_e and N_n are the number density of electrons and neutrons respectively with $N_e \simeq N_n$ in earth matter. The δc_{ij}'s are CPT violating terms. Different angular values for unitary matrix U_b are checked in [43]. In our work we have considered $U = U_b$. Hamiltonian H_f can be diagonalized to H_D by an unitary matrix $\tilde{U}$. This can be expressed as

$$H_D = \tilde{U}^\dagger H_f \tilde{U} \tag{5}$$

The matrix elements $[H_D]_{ii}$ will represent the eigenvalues of H_f. Full analytical expressions for neutrino oscillation probabilities are developed in this work by using time independent perturbation theory. In an attempt to apply perturbation we have defined few oscillation parameters in terms of perturbative parameter η, where $\eta = 0.18$. The neutrino oscillation parameters can be rewritten as

$$\theta_{14} \equiv \chi_{14}\eta$$
$$\theta_{24} \equiv \chi_{24}\eta$$
$$\theta_{34} \equiv \chi_{34}\eta$$
$$\theta_{13} \equiv \chi_{13}\eta$$
$$\hat{\theta_{23}} \simeq \theta_{23} - 1/\sqrt{2} \equiv \chi_{23}\eta$$

We treat $\dfrac{\Delta m^2_{21}}{\Delta m^2_{31}} \approx O(\eta^2)$. Now the Hamiltonian H_f can be written as

$$H_f = \frac{\Delta m^2_{31}}{2E}\left[H_0 + H_1(\eta) + H_2(\eta^2) + O(\eta^3)\right] \tag{6}$$

where H_0, H_1 and H_2 are the hamiltonians corresponding to zeroth, first and second order in η respectively. The evolution equation for neutrino oscillation probability is defined as

$$P_{\alpha\beta} = \mid S_{\beta\alpha}(t, t_0) \mid^2 \tag{7}$$

where $S(t, t_0)$ is the evolution matrix of neutrino which is also called oscillation probability amplitude

$$\mid \nu(t) > = S(t, t_0) \mid \nu(t_0) > \tag{8}$$

The evolution matrix of neutrinos in terms of eigenvalues of H_f can be written as

$$S_{\beta\alpha}(t,t_0) = \sum_{i=1}^{4} (\tilde{U}_{\alpha i})^* \tilde{U}_{\beta i} e^{-i E_i L} \tag{9}$$

where $L \equiv t - t_0$.

From equation (7) the neutrino oscillation probability $P_{\alpha\beta}$ from flavor α to flavor β can be written as

$$P_{\alpha\beta} = |\sum_{i=1}^{4} (\tilde{U}_{\alpha i})^* (\tilde{U}_{\beta i}) e^{-i E_i L}|^2 \tag{10}$$

This is the general form of equation for neutrino oscillation probability.

3. T violation in (3 + 1) framework

In neutrino oscillations the flavor conversion probabilities from flavor α to flavor β can be written as

$$P_{\nu_\alpha \longrightarrow \nu_\beta} = \delta_{ij} - 4 \sum_{i>j} Re\left[\tilde{U}_{\alpha i} \tilde{U}^*_{\alpha j} \tilde{U}^*_{\beta i} \tilde{U}_{\beta j}\right] \sin^2 \Delta_{ij} + 2 \sum_{i>j} Im\left[\tilde{U}_{\alpha i} \tilde{U}^*_{\alpha j} \tilde{U}^*_{\beta i} \tilde{U}_{\beta j}\right] \sin 2\Delta_{ij} \tag{11}$$

Redefining the above probability equation as sum of $P_{CP-even}$ and P_{CP-odd} terms

$$P_{\alpha\beta} = P_{(\nu_\alpha \to \nu_\beta)} = P_{CP-even}(\nu_\alpha \to \nu_\beta) + P_{CP-odd}(\nu_\alpha \to \nu_\beta) \tag{12}$$

CP even terms are CP conserving and can be written as

$$P_{(\nu_\alpha \to \nu_\beta)} = P_{(\bar{\nu}_\alpha \to \bar{\nu}_\beta)} = \delta_{ij} - 4 \sum_{i>j} Re(\tilde{U}_{\alpha i} \tilde{U}^*_{\beta i} \tilde{U}^*_{\alpha j} \tilde{U}_{\beta j}) \sin^2 \Delta_{ij} \tag{13}$$

CP odd terms are CP violating and can be written as

$$P_{(\nu_\alpha \to \nu_\beta)} = -P_{(\bar{\nu}_\alpha \to \bar{\nu}_\beta)} = 2 \sum_{i>j} Im(\tilde{U}_{\alpha i} \tilde{U}^*_{\beta i} \tilde{U}^*_{\alpha j} \tilde{U}_{\beta j}) \sin 2\Delta_{ij} \tag{14}$$

Assuming CPT to be conserved, the magnitude of CP violation (ΔP_{CP}) will be equal to the magnitude of T violation (ΔP_T), i.e.

$$|\Delta P_{CP}| = |\Delta P_T| \tag{15}$$

therefore we can write

$$P_{(\nu_\alpha \to \nu_\beta)} - P_{(\bar{\nu_\alpha} \to \bar{\nu_\beta})} \equiv P_{(\nu_\alpha \to \nu_\beta)} - P_{(\nu_\beta \to \nu_\alpha)} \tag{16}$$

When neutrinos passes through the earth matter, the interaction of neutrinos with matter gives rise to an extra potential. This potential is positive for neutrinos and negative for antineutrinos, leading to different energy eigenvalues of hamiltonian for neutrinos and antineutrinos. Further, this difference in hamiltonian for ν's and $\bar{\nu}$'s give rise to fake (extrinsic) CP violation. Hence, check on T violation appears to be a better choice in the presence of matter. From equation (16) the T violation can be looked upon as

$$(\Delta P_T)_{\alpha\beta} = P(\nu_\alpha \to \nu_\beta) - P(\bar{\nu_\alpha} \to \bar{\nu_\beta}) \equiv 4 \sum_{i>j} Im(\tilde{U}_{\alpha i} \tilde{U}^*_{\beta i} \tilde{U}^*_{\alpha j} \tilde{U}_{\beta j}) \sin 2\Delta_{ij} \tag{17}$$

If we consider $\tilde{U}_{\alpha j}\tilde{U}^{*}_{\beta j} = \tilde{V}_{j}^{\alpha\beta}$ and $\Delta_{ij} = 2\Delta\tilde{E}_{jk}/L = 2(\tilde{E}_j - \tilde{E}_k)/L$ the above equation becomes

$$(\Delta P_T)_{\alpha\beta} \equiv 4\sum_{j<k} Im(\tilde{V_j}^{\beta\alpha}\tilde{V_k}^{\beta\alpha^*})\sin(\Delta\tilde{E}_{jk}L) \tag{18}$$

The term $Im(\tilde{V_j}^{\beta\alpha}\tilde{V_k}^{\beta\alpha^*})$ is known as Jarlskog factor and $\tilde{E}'_j s$ are energy eigenvalues of hamiltonian in matter.

$$\begin{aligned}(\Delta P_T)_{\alpha\beta} = {} & 4Im(\tilde{V_1}^{\beta\alpha}\tilde{V_2}^{\beta\alpha^*})\sin(\Delta\tilde{E}_{12}L) + 4Im(\tilde{V_1}^{\beta\alpha}\tilde{V_3}^{\beta\alpha^*})\sin(\Delta\tilde{E}_{13}L) \\ & + 4Im(\tilde{V_2}^{\beta\alpha}\tilde{V_3}^{\beta\alpha^*})\sin(\Delta\tilde{E}_{23}L) + 4Im(\tilde{V_1}^{\beta\alpha}\tilde{V_4}^{\beta\alpha^*})\sin(\Delta\tilde{E}_{14}L) \\ & + 4Im(\tilde{V_2}^{\beta\alpha}\tilde{V_4}^{\beta\alpha^*})\sin(\Delta\tilde{E}_{24}L) + 4Im(\tilde{V_3}^{\beta\alpha}\tilde{V_4}^{\beta\alpha^*})\sin(\Delta\tilde{E}_{34}L)\end{aligned} \tag{19}$$

The energy eigenvalues in matter can be connected to the energy eigenvalues in vacuum by the relations $\tilde{E}_1 = \Delta E_{31}$, $\tilde{E}_2 = 0$, $\tilde{E}_3 = A_e$ and $\tilde{E}_4 = \Delta E_{41}$. The terms $\tilde{V_1}^{\alpha\beta}$, $\tilde{V_2}^{\alpha\beta}$, $\tilde{V_3}^{\alpha\beta}$, $\tilde{V_4}^{\alpha\beta}$ in matter can be calculated with the help of the terms $V_1^{\alpha\beta}$, $V_2^{\alpha\beta}$, $V_3^{\alpha\beta}$, $V_4^{\alpha\beta}$ in vacuum (where $V_j^{\alpha\beta} = U_{\alpha j}U^{*}_{\beta j}$) using the following expressions [44].

$$\tilde{V_1}^{\beta\alpha} = -\Delta\tilde{E}_{21}^{-1}\Delta\tilde{E}_{31}^{-1}\{V_4^{\beta\alpha}\tilde{E}_2\tilde{E}_3 + (\tilde{E}_2+\tilde{E}_3)R^{\beta\alpha} + S^{\beta\alpha}\} \tag{20}$$

$$\tilde{V_2}^{\beta\alpha} = \Delta\tilde{E}_{21}^{-1}\Delta\tilde{E}_{32}^{-1}\{V_4^{\beta\alpha}\tilde{E}_3\tilde{E}_1 + (\tilde{E}_3+\tilde{E}_1)R^{\beta\alpha} + S^{\beta\alpha}\} \tag{21}$$

$$\tilde{V_3}^{\beta\alpha} = -\Delta\tilde{E}_{31}^{-1}\Delta\tilde{E}_{32}^{-1}\{V_4^{\beta\alpha}\tilde{E}_1\tilde{E}_2 + (\tilde{E}_1+\tilde{E}_2)R^{\beta\alpha} + S^{\beta\alpha}\} \tag{22}$$

$$\tilde{V_4}^{\beta\alpha} = V_4^{\beta\alpha} \tag{23}$$

where

$$R^{\beta\alpha} = \{A(V_4^{ee} + V_4^{ss}/2) - A_{\alpha\alpha} - A_{\beta\beta}\}V_4^{\beta\alpha} + \Delta E_{31}V_3^{\beta\alpha} + \Delta E_{21}V_2^{\beta\alpha} \tag{24}$$

$$\begin{aligned}S^{\beta\alpha} = {} & V_4^{\beta\alpha}\{A_{\alpha\alpha}^2 + A_{\alpha\alpha}A_{\beta\beta} + A_{\beta\beta}^2 - A(A_{\alpha\alpha}+A_{\beta\beta})(V_4^{ee}+V_4^{ss}/2)\} \\ & - \Delta E_{31}(\Delta E_{31} + A_{\alpha\alpha} + A_{\beta\beta})V_3^{\beta\alpha} - \Delta E_{21}(\Delta E_{21} + A_{\alpha\alpha} + A_{\beta\beta})V_2^{\beta\alpha} \\ & + A\Delta E_{31}(V_4^{\beta e}V_3^{e\alpha} + V_3^{\beta e}V_4^{e\alpha} + V_4^{\beta s}V_3^{s\alpha} + V_3^{\beta s}V_4^{s\alpha}) \\ & + A\Delta E_{21}(V_4^{\beta e}V_2^{e\alpha} + V_2^{\beta e}V_4^{e\alpha} + V_4^{\beta s}V_2^{s\alpha} + V_2^{\beta s}V_4^{s\alpha})\end{aligned} \tag{25}$$

$A_\alpha = A_e\delta_{\alpha e} - A_n\delta_{\alpha s}$ is the diagonal element of the matter potential matrix in four neutrino scheme and A is the diagonal element of matter potential matrix in three neutrino scheme. Since T violating effects can only be studied in appearance channels so $\alpha \neq \beta$. In an effort to put constraints on ΔP_T we have studied two appearance channels. These are $\nu_e \to \nu_\mu$ (golden channel) and $\nu_\mu \to \nu_\tau$ (discovery channel).

For T violation, probability difference expression for the golden channel can be expressed as

$$\begin{aligned}(\Delta P_T)_{\mu e} = {} & \frac{-4}{(\Delta m_{31}^2/2E)^2\frac{A_e}{2E}(\frac{A_e}{2E} - \Delta m_{31}^2/2E)} \times \\ & [\frac{A_e}{2E}R^{e\mu} + S^{e\mu}][s_{14}c_{14}s_{24}\frac{A_e}{2E}\Delta m_{31}^2/2E \\ & + (\frac{A_e}{2E} + \Delta m_{31}^2/2E)R^{e\mu} + S^{e\mu}]\sin\Delta m_{31}^2 L/2E\end{aligned}$$

$$
\begin{aligned}
&+\frac{4}{(-\Delta m^2_{31}/2E)\frac{A_e}{2E}(\frac{A_e}{2E}-\Delta m^2_{31}/2E)^2}\times \\
&[\frac{A_e}{2E}R^{e\mu}+S^{e\mu}][(\Delta m^2_{31}/2E)R^{e\mu}+S^{e\mu}]\sin(\Delta m^2_{31}/2E-\frac{A_e}{2E})L+ \\
&\frac{4}{(-\Delta m^2_{31}/2E)(\frac{A_e}{2E}-\Delta m^2_{31}/2E)(\frac{A_e}{2E})^2}[s_{14}c_{14}s_{24}\frac{A_e}{2E}\Delta m^2_{31}/2E \\
&+(\frac{A_e}{2E}+\Delta m^2_{31}/2E)R^{e\mu} \\
&+S^{e\mu}]\times[(\Delta m^2_{31}/2E)R^{e\mu}+S^{e\mu}]\sin\frac{A_e}{2E}L
\end{aligned}
\tag{26}
$$

Since large value of Δm^2_{41} gives rise to rapid oscillations, hence Δm^2_{41} terms can be averaged out. Solving the above expression up to the power s^4_{ij} we get

$$
\begin{aligned}
(\Delta P_T)_{\mu e} &= 4c_{13}c^2_{14}c_{24}s_{13}s_{23}s_{14}s_{24}\sin(\delta_2-\delta_3)\frac{\Delta_e}{(\Delta_e-\Delta_{31})}\sin\Delta m^2_{31}L/2E \\
&\quad+4c_{13}c^2_{14}c_{24}s_{13}s_{23}s_{14}s_{24}\sin(\delta_2-\delta_3)\frac{\Delta^2_{31}}{\Delta_e(\Delta_e-\Delta_{31})}\sin 2\Delta_e
\end{aligned}
\tag{27}
$$

$$
\begin{aligned}
(\Delta P_T)_{\mu e} &= 4c_{13}c^2_{14}c_{24}s_{13}s_{23}s_{14}s_{24}\sin(\delta_2-\delta_3)[\frac{\Delta_e}{(\Delta_e-\Delta_{31})}\sin\Delta m^2_{31}L/2E \\
&\quad+\frac{\Delta^2_{31}}{\Delta_e(\Delta_e-\Delta_{31})}\sin 2\Delta_e]
\end{aligned}
\tag{28}
$$

$\Delta_e = A_e L/4E$ is matter dependent term. Any change in Δ_e will change the value of $(\Delta P_T)_{\mu e}$.

Further we have developed equation of ΔP_T for discovery channel. The discovery channel is not very useful in the standard three neutrino flavor framework, nevertheless while studying physics beyond three active neutrino flavor framework, study of this channel becomes important. For discovery channel ($\nu_\mu \to \nu_\tau$) the probability difference is given as

$$
\begin{aligned}
(\Delta P_T)_{\mu\tau} &= \frac{-4}{(\Delta m^2_{31}/2E)^2\frac{A_e}{2E}(\frac{A_e}{2E}-\Delta m^2_{31}/2E)}\times \\
&\quad[\frac{A_e}{2E}R^{\tau\mu}+S^{\tau\mu}][c^2_{14}c_{24}s_{24}s_{34}\frac{A_e}{2E}\Delta m^2_{31}/2E \\
&\quad+(\frac{A_e}{2E}+\Delta m^2_{31}/2E)R^{\tau\mu}+S^{\tau\mu}]\sin\Delta m^2_{31}L/2E \\
&\quad+\frac{4}{(-\Delta m^2_{31}/2E)\frac{A_e}{2E}(\frac{A_e}{2E}-\Delta m^2_{31}/2E)^2}\times \\
&\quad[\frac{A_e}{2E}R^{\tau\mu}+S^{\tau\mu}][(\Delta m^2_{31}/2E)R^{\tau\mu}+S^{\tau\mu}]\sin(\Delta m^2_{31}/2E-\frac{A_e}{2E})L+ \\
&\quad\frac{4}{(-\Delta m^2_{31}/2E)(\frac{A_e}{2E}-\Delta m^2_{31}/2E)(\frac{A_e}{2E})^2}[c^2_{14}c_{24}s_{24}s_{34}\frac{A_e}{2E}\Delta m^2_{31}/2E \\
&\quad+(\frac{A_e}{2E}+\Delta m^2_{31}/2E)R^{\tau\mu} \\
&\quad+S^{\tau\mu}]\times[(\Delta m^2_{31}/2E)R^{\tau\mu}+S^{\tau\mu}]\sin\frac{A_e}{2E}L
\end{aligned}
\tag{29}
$$

Solving the above expression up to the power s_{ij}^4 we get,

$$(\Delta P_T)_{\mu\tau} = 4c_{13}^2c_{14}^2c_{23}c_{24}^2c_{34}s_{23}s_{24}s_{34}\sin(\delta_3)\frac{\Delta_e}{\Delta_{31}}\sin\Delta m_{31}^2 L/2E - 4c_{13}^2c_{14}^2c_{23}c_{24}^2c_{34}s_{23}s_{24}s_{34}\sin(\delta_3)\frac{\Delta_{31}}{\Delta_e}\sin 2\Delta_e \tag{30}$$

$$(\Delta P_T)_{\mu\tau} = 4c_{13}^2c_{14}^2c_{23}c_{24}^2c_{34}s_{23}s_{24}s_{34}\sin(\delta_3)[\frac{\Delta_e}{\Delta_{31}}\sin\Delta m_{31}^2 L/2E - \frac{\Delta_{31}}{\Delta_e}\sin 2\Delta_e] \tag{31}$$

The expression of ΔP_T for three neutrino framework [45] is given by

$$\Delta(P_T)_{3\times3} \approx 4c_{12}c_{13}^2c_{23}s_{12}s_{13}s_{23}\sin\delta \tag{32}$$

Keeping the best fit values of neutrino oscillation parameters and assigning maximum value to Dirac phases i.e. keeping mod of sin of Dirac phases to be unity will lead us to maximum value of ΔP_T. This assumption will render the maximum limit on the bounds which can be imposed on T violation arising due to the presence of Dirac phases if all other oscillation parameters are known with utmost accuracy. From equation (32) we get the value of $(\Delta P_T)_{max} = 0.137$ for three neutrino flavor framework [46]. This value is independent of the selection of probing channel and presence of matter effects. Whereas in four flavor framework it will depend on the selection of channel through which we want to probe CP or T violation and it will vary with matter effects too. Within four flavor neutrino framework the magnitude of ΔP_T will depend on active flavor neutrino mixing angles (known with accuracy), sterile neutrino mixing angles (still needs better bounds), matter effects, baseline, energy and Dirac phases (not known). Imposition of constraints on Dirac phase (three neutrino flavor) or phases (four neutrino flavor) is still in research phase.

The probability differences $(\Delta P_T)_{4\times4}$ in neutrino sector are represented by equations (28) and (31) for $\nu_\mu \to \nu_e$ and $\nu_\mu \to \nu_\tau$ channels respectively. The values of sterile parameters used in the above mentioned equations are taken from

(i) long baseline neutrino oscillation experiments [47]

$$\theta_{14} \lesssim 6.7^\circ,\ \theta_{24} \lesssim 3.3^\circ \text{ and } \theta_{34} \lesssim 6.3^\circ$$

(ii) short baseline reactor and atmospheric experiments [48,49]

$$\theta_{14} \lesssim 10^\circ,\ \theta_{24} \lesssim 12^\circ \text{ and } \theta_{34} \lesssim 28^\circ$$

The variations in $(\Delta P_T)_{\mu e}$ and $(\Delta P_T)_{\mu\tau}$ are checked along the baseline for two different energies i.e. 4 GeV and 50 GeV. Plot (a) of Fig. 1 reflects very small variations in $(\Delta P_T)_{4\times4}$ in comparison to $(\Delta P_T)_{3\times3}$ along golden channel, when checked for two different energies and two sets of sterile parameter values. Plot (b) of Fig. 1 reflects a reasonable variation in $(\Delta P_T)_{4\times4}$ in comparison to $(\Delta P_T)_{3\times3}$ along discovery channel, when checked for 50 GeV energy with sterile parameters values taken from reactor+atmospheric experiments. The $\nu_\mu \longrightarrow \nu_\tau$ comes up as the promising channel to observe the signatures of T violation. From the analysis we conclude that neutrino factory operating at 50 GeV has the potential to capture the signatures of T violation through $\nu_\mu \longrightarrow \nu_\tau$ channel if true sterile parameter values are equal to that taken from reactor+atmospheric experiments. At the same time if the upcoming neutrino experimental setups capture ΔP_T value above 0.137 then to explain the physics behind this enalargement, we have to move beyond the standard three active neutrino physics.

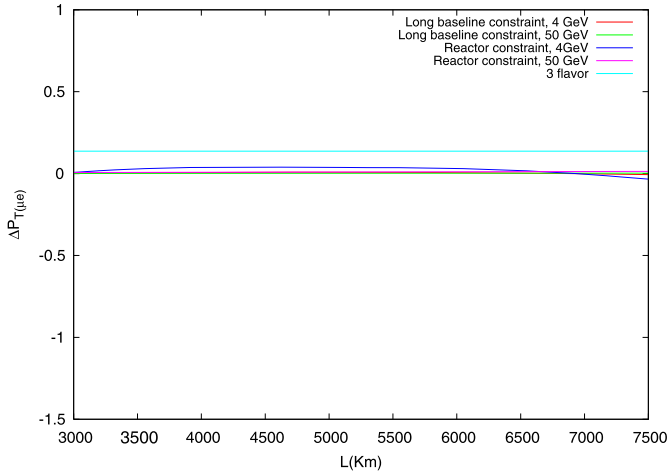

(a)Variation in $(\Delta P_T)_{\mu e}$ along the baseline

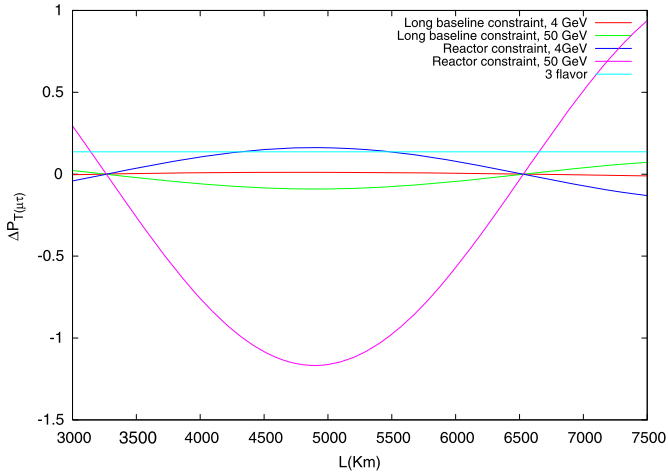

(b)Variation in $(\Delta P_T)_{\mu\tau}$ along the baseline

Fig. 1. The variation in ΔP_T with baseline for two different appearance channels.

4. CPT violation in 3 + 1 scheme

CPT invariance is one of the most fundamental symmetries of nature. CPT conservation indicates the invariance in the properties of physical quantities under the discrete transformations such as charge conjugation (C), parity inversion (P) and time reversal (T) along with the invariance under Lorentz transformation. CPT invariance is one of the symmetries of local quantum field theory which implies that there is an important relation between CPT invariance and Lorentz invariance. If CPT invariance is violated, Lorentz invariance must violate but if Lorentz invariance is violated it is not necessary that CPT invariance must violate. In our work $\nu_\mu \to \nu_\mu$ disappearance channel is probed to check CPT violation. The CPT violating probability difference can be written as

$$\triangle P^{CPT}_{\alpha\beta} = P_{\alpha\beta} - P_{\bar{\beta}\bar{\alpha}} \tag{33}$$

The intrinsic CPT violation arises due to the non-invariance of standard model extension lagrangian under CPT transformation. A standard model extension hamiltonian H_f for neutrinos, containing CPT violating terms is defined by equation (4) and the general form of neutrino oscillation probability is mentioned in equation (10). The terms $\tilde{U}_{\alpha i}, \tilde{U}^*_{\alpha j}, \tilde{U}^*_{\beta i}$ and $\tilde{U}_{\beta j}$ of the expression (10) are the elements of the unitary matrix $\tilde{U}$. The construction of unitary matrix $\tilde{U}$ with the help of eigenvalues and eigenvectors of hamiltonian H_0, H_1 and H_2 is mentioned in the Appendix A. After the formation of unitary matrix $\tilde{U}$, we have developed the neutrino oscillation probability equations up to second order in η. Since Δm^2_{41} is large, so we average out the effects produced due to Δm^2_{41} in the probability equations. Neutrino oscillation probabilities for different oscillation channels containing CPT violating parameters can be developed as

$$P_{ee} = 1 - 2{\theta_{14}}^2 - 4{\theta_{13}}^2(\Delta_{31} + \delta c_{31} L/2)^2 \frac{\sin^2(\Delta_{31} + \delta c_{31} L/2 - \Delta_e)}{(\Delta_{31} + \delta c_{31} L/2 - \Delta_e)^2} \tag{34}$$

$$P_{e\mu} = P_{e\tau} = 2\theta^2_{13}(\Delta_{31} + \delta c_{31} L/2)^2 \frac{\sin^2(\Delta_{31} + \delta c_{31} L/2 - \Delta_e)}{(\Delta_{31} + \delta c_{31} L/2 - \Delta_e)^2} \tag{35}$$

$$\begin{aligned} P_{\mu\mu} = {} & 1 - 2\theta^2_{24}\cos^2(\Delta_{31} + \delta c_{31} L/2) - (1 - 8\hat{\theta^2_{23}})\sin^2(\Delta_{31} + \delta c_{31} L/2) \\ & + (c^2_{12}\Delta_{12} - 2\theta_{24}\theta_{34}\cos\delta_3\Delta_n)\sin 2(\Delta_{31} + \delta c_{31} L/2) \\ & + \frac{\theta^2_{13}(\Delta_{31} + \delta c_{31} L/2)}{(\Delta_{31} + \delta c_{31} L/2 - \Delta_e)^2}[2(\Delta_{31} + \delta c_{31} L/2)\sin\Delta_e\cos(\Delta_{31} + \delta c_{31} L/2) \\ & \sin(\Delta_{31} + \delta c_{31} L/2 - \Delta_e) - (\Delta_{31} + \delta c_{31} L/2 - \Delta_e)\Delta_e \sin 2\Delta_{31} + \delta c_{31} L/2] \end{aligned} \tag{36}$$

$$\begin{aligned} P_{\mu\tau} = {} & \sin^2(\Delta_{31} + \delta c_{31} L/2) - (8\hat{\theta^2_{23}} + \theta^2_{24} + \theta^2_{34})\sin^2(\Delta_{31} + \delta c_{31} L/2) \\ & - (c^2_{12}\Delta_{12} + 2\theta_{24}\theta_{34}\cos\delta_3\Delta_n)\sin 2(\Delta_{31} + \delta c_{31} L/2) - \frac{s^2_{13}(\Delta_{31} + \delta c_{31} L/2)}{(\Delta_{31} + \delta c_{31} L/2 - \Delta_e)^2} \\ & [2(\Delta_{31} + \delta c_{31} L/2)\sin(\Delta_{31} + \delta c_{31} L/2)\cos\Delta_e \sin(\Delta_{31} + \delta c_{31} L/2 - \Delta_e) \\ & - (\Delta_{31} + \delta c_{31} L/2 - \Delta_e)\Delta_e \sin 2(\Delta_{31} + \delta c_{31} L/2)] \\ & + \theta_{24}\theta_{34}\sin\delta_3 \sin 2(\Delta_{31} + \delta c_{31} L/2) \end{aligned} \tag{37}$$

$$P_{\mu s} = 2\theta^2_{24} + (\theta^2_{34} - \theta^2_{24})\sin^2(\Delta_{31} + \delta c_{31} L/2) - \theta_{24}\theta_{34}\sin\delta_3 \sin 2(\Delta_{31} + \delta c_{31} L/2) \tag{38}$$

For small angles ($\theta_{ij} \simeq \sin\theta_{ij} \simeq s_{ij}$) these oscillation probabilities can be written as

$$P_{ee} = 1 - 2{s_{14}}^2 - 4{s_{13}}^2(\Delta_{31} + \delta c_{31} L/2)^2 \frac{\sin^2(\Delta_{31} + \delta c_{31} L/2 - \Delta_e)}{(\Delta_{31} + \delta c_{31} L/2 - \Delta_e)^2} \tag{39}$$

$$P_{e\mu} = P_{e\tau} = 2s^2_{13}(\Delta_{31} + \delta c_{31} L/2)^2 \frac{\sin^2(\Delta_{31} + \delta c_{31} L/2 - \Delta_e)}{(\Delta_{31} + \delta c_{31} L/2 - \Delta_e)^2} \tag{40}$$

$$\begin{aligned} P_{\mu\mu} = {} & 1 - 2s^2_{24}\cos^2(\Delta_{31} + \delta c_{31} L/2) - (1 - 8\hat{s^2_{23}})\sin^2(\Delta_{31} + \delta c_{31} L/2) \\ & + (c^2_{12}\Delta_{12} - 2s_{24}s_{34}\cos\delta_3\Delta_n)\sin 2(\Delta_{31} + \delta c_{31} L/2) + \frac{s^2_{13}(\Delta_{31} + \delta c_{31} L/2)}{(\Delta_{31} + \delta c_{31} L/2 - \Delta_e)^2} \\ & \times [2(\Delta_{31} + \delta c_{31} L/2)\sin\Delta_e\cos(\Delta_{31} + \delta c_{31} L/2)\sin(\Delta_{31} + \delta c_{31} L/2 - \Delta_e) - \\ & (\Delta_{31} + \delta c_{31} L/2 - \Delta_e)\Delta_e \sin 2(\Delta_{31} + \delta c_{31} L/2)] \end{aligned} \tag{41}$$

Table 1
Systematics.

Systematic uncertainties	Values
Flux normalization	2%
Fiducial mass errors for near detector	0.6%
Fiducial mass errors for far detector	0.6%
Energy calibration error for near detector	0.5%
Energy calibration error for far detector	0.5
Shape error	10%
Backgrounds	10^{-4}

$$P_{\mu\tau} = \sin^2(\Delta_{31} + \delta c_{31} L/2) - (8s^2_{23} + \hat{s^2_{24}} + s^2_{34}) \sin^2(\Delta_{31} + \delta c_{31} L/2) - (c^2_{12}\Delta_{12} + 2s_{24}s_{34}\cos\delta_3\Delta_n) \sin 2(\Delta_{31} + \delta c_{31} L/2) - \frac{s^2_{13}(\Delta_{31} + \delta c_{31} L/2)}{(\Delta_{31} + \delta c_{31} L/2 - \Delta_e)^2} \times [2(\Delta_{31} + \delta c_{31} L/2)\sin(\Delta_{31} + \delta c_{31} L/2)\cos\Delta_e \sin(\Delta_{31} + \delta c_{31} L/2 - \Delta_e) - (\Delta_{31} + \delta c_{31} L/2 - \Delta_e)\Delta_e \sin 2(\Delta_{31} + \delta c_{31} L/2)] + s_{24}s_{34}\sin\delta_3 \sin 2(\Delta_{31} + \delta c_{31} L/2) \quad (42)$$

$$P_{\mu s} = 2s^2_{24} + (s^2_{34} - s^2_{24}) \sin^2(\Delta_{31} + \delta c_{31} L/2) - s_{24}s_{34}\sin\delta_3 \sin 2(\Delta_{31} + \delta c_{31} L/2) \quad (43)$$

In order to analyze CPT violation at probability level in four flavor neutrino framework the value of $\Delta P^{CPT}_{\alpha\beta}$ considered in our analysis is given by

$$\triangle P^{CPT}_{\alpha\beta} = [(P_{\alpha\beta})_{4\nu}]_{\delta c_{ij}\neq 0} - [(P_{\alpha\beta})_{4\nu}]_{\delta c_{ij}=0} \quad (44)$$

Neutrino factory setup considered for analyzing CPT violation is taken from the references [50–53] and [54]. The experimental setup and detector specifications considered in our analysis are mentioned below. Neutrino factory setup consist of 1.4×10^{21} useful muon decays per polarity, with parent muon energy $E_\mu = 50$ GeV. We have done our analysis for 10 years running of neutrino factory. In particle physics meaningful observations always demands a detector with very good energy and angular resolutions. This view point lead us to select Liquid Argon detector for particle detection. The energy resolution of the detector for muon is $\sigma(\text{GeV}) = 0.20/\sqrt{E_\nu(\text{GeV})}$.

A near detector is placed at a distance 20 m from the end of the decay straight of the muon storage ring. Effective baseline (L_{eff}) is used in place of baseline (L), which is calculated using $L_{eff} = \sqrt{d(d+s)}$ [55]. Fiducial mass of near detector is 200 tons. Presence of near detector will minimize the systematic uncertainties in our observations.

A 50 Kt far detector is placed at a distance of 7500 km. The systematic uncertainties considered for this analysis are given in Table 1. An uncertainty of 5% on matter density [56,57] is also considered in our work. The simulated environment of the neutrino factory is created with the help of GLoBES [58,59]. The analytical equations for four flavor neutrino conversion probabilities derived in this work are defined in the probability engine of the software. The best fit values of oscillation parameters [47,60] are mentioned in Table 2. Sterile parameter values mentioned in the Table 2 represents best fit values for $\Delta m^2_{41} = 0.1$ eV^2.

The constraints on CPT violating parameters δc_{21} and δc_{31} within two and three neutrino frameworks are mentioned in references [43,61–65] and [66]. In present work we are trying to check the neutrino factory potential to capture CPT violating signatures in presence of sterile neutrino. As the mass hierarchy determination is yet in the phase of research, therefore in an attempt

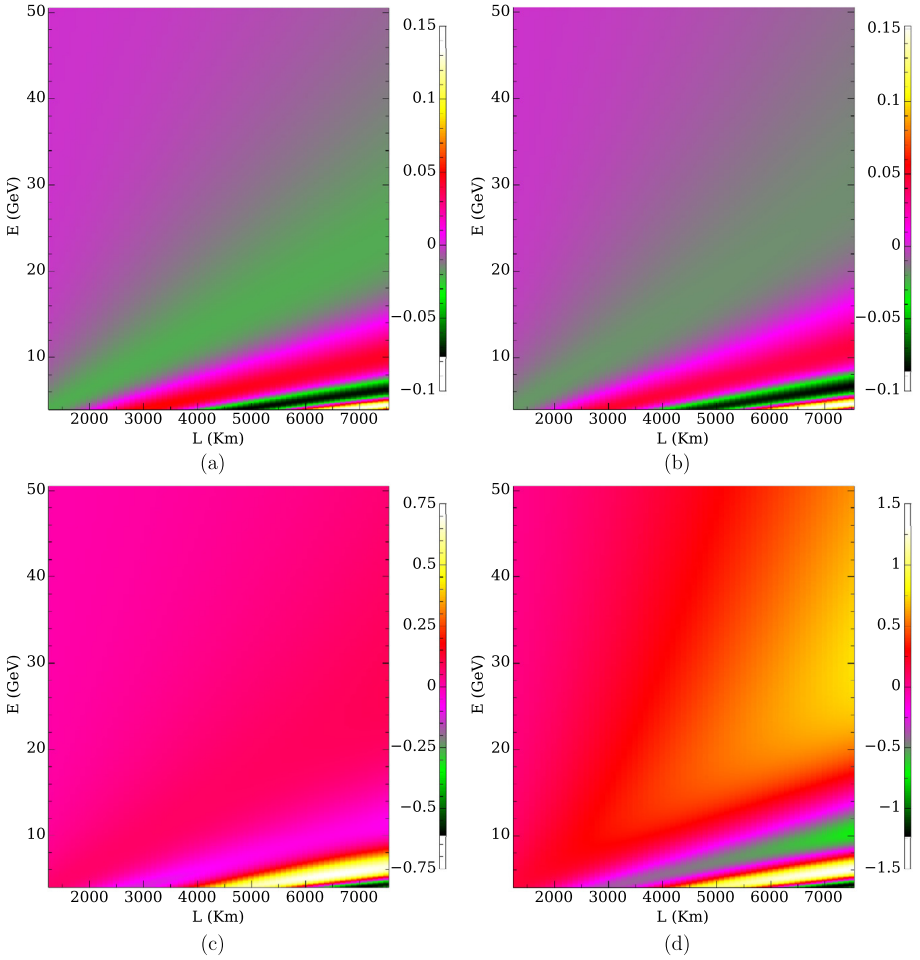

Fig. 2. The oscillographs (a) and (b) demonstrate the variation of $\Delta P^{CPT}_{\mu\mu}$ with baseline and energy for normal hierarchy whereas (c) and (d) illustrate the same for inverted hierarchy. For the oscillographs (a) and (c) the values of sterile parameters are selected from long baseline experiments while for (b) and (d) the values of sterile parameters are taken from reactor and atmospheric experiments.

Table 2
Best fit values of the oscillation parameters.

Parameter	Best fit values
θ_{12}	34.4°
θ_{13}	8.50°
θ_{23}	45.0°
θ_{14}	6.7°; 10°
θ_{24}	3.3°; 12°
θ_{34}	6.3°; 28°
Δm^2_{21}	8×10^{-5} eV^2
Δm^2_{31}	2.5×10^{-3} eV^2

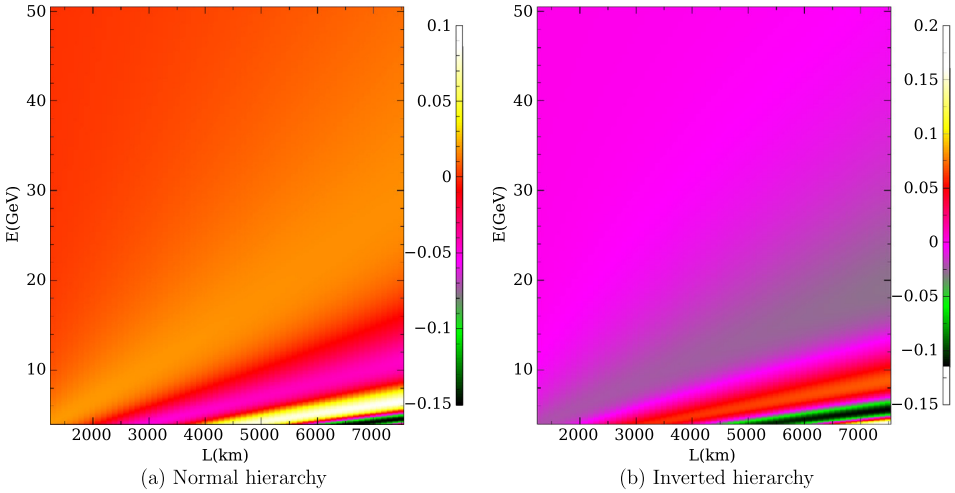

Fig. 3. The oscillographs demonstrate the variation of $\Delta P^{CPT}_{\bar{\mu}\bar{\mu}}$ with baseline and energy. The values of sterile parameters are selected from reactor+atm experiments. Left and right oscillographs are for normal and inverted hierarchies respectively.

to make this work relevant we have analyzed CPT invariance for both the mass hierarchies. Initially CPT violating signatures are checked at probability level. The value of $\Delta P^{CPT}_{\alpha\beta}$ is estimated by substituting equation (41) in equation (44) for the channel $\nu_\mu \to \nu_\mu$. The variation in $\Delta P^{CPT}_{\mu\mu}$ and $\Delta P^{CPT}_{\bar{\mu}\bar{\mu}}$ with baseline and energy are shown in Fig. 2 and Fig. 3 oscillographs respectively. The total CPT violation captured by any experiment will be the sum of extrinsic CPT violation (CPT violation arising due to matter effects) and intrinsic or genuine CPT violation (which we are probing in present work). In an endeavor to constraint intrinsic CPT violating parameters we must look for places where extrinsic CPT violation is negligible or very low. With three active neutrinos the extrinsic CPT violation is checked in reference [67] whereas with 3 (active) + 1 (sterile) neutrinos it is checked in reference [68]. Equation (44) of our work will check the presence of pure CPT violation arising in the presence of sterile neutrino at probability level. The values of CPT violating parameters considered while plotting oscillographs are $\delta c_{31} = 4 \times 10^{-23}$ GeV and $\delta c_{21} = 3 \times 10^{-23}$ GeV. Looking at normal and inverted hierarchy oscillographs (Fig. 2) we can observe the presence of pure CPT violating signatures at shorter baselines i.e. from 1300 km to 2000 km for 4 GeV–6 GeV energies. The references [67,68], which speak about extrinsic CPT violation, have recorded very weak or almost negligible signatures of extrinsic CPT violation at the above mentioned energies and baselines. Hence baselines from 1300 km to 2000 km with neutrino energies in the range 4 GeV–6 GeV are favorable for probing CPT violation with neutrino factory. In Fig. 2 while looking at normal hierarchy oscillographs we observe $\Delta P^{CPT}_{\mu\mu} = -0.05$ along baselines 4000 km to 7500 km for energies 14 GeV–30 GeV. The inverted hierarchy oscillographs of the same Figure captures $\Delta P^{CPT}_{\mu\mu} = 0.25$ and 1 for sterile parameters taken from long baseline experiments and reactor+atmospheric experiments respectively. This probability difference can be observed for baselines from 4500 km to 7500 km and for energies between 14 GeV–50 GeV.

After examining the presence of pure CPT violation at probability level we go ahead to observe the signatures of the same with proposed neutrino experiments i.e. neutrino factory. The specifications of neutrino factory considered in our work are mentioned earlier. Liquid argon

detector seems a reasonable choice to grab the signatures of leptons in the considered energy range. The rate (event) level analysis depends on mathematical formulation (oscillation probability), physics (types of interactions) and R & D (source properties and detector properties) of the experiment. Looking at equations (34) to (44) we found that CPT violating term δc_{21} appears with Δm^2_{21} term and CPT violating term δc_{31} term appears with Δm^2_{31} term. The solar and atmospheric mass square difference (Δm^2_{21} and Δm^2_{31}) are of the order of 10^{-23} and 10^{-21} (in GeV^2) respectively. Hence, any change in mass terms due to the presence of CPT violating parameter will be better observed in δc_{31} term.

To hook CPT violating impression with neutrino factory we have investigated some observable parameters like R, $\triangle R$ and asymmetry factor. These terms are defined by equations (45) and (46). The ratio R and ratio difference ΔR are examined as

$$R = \frac{N(\nu_\mu \to \nu_\mu)}{N(\bar{\nu_\mu} \to \bar{\nu_\mu})}; \triangle R = (R_{4\nu})_{\delta c_{ij} \neq 0} - (R_{4\nu})_{\delta c_{ij}=0} \tag{45}$$

where $N(\nu_\mu \to \nu_\mu)$ denotes number of muon neutrinos reaching at detector as muon neutrinos and producing a μ^+ lepton and $N(\bar{\nu_\mu} \to \bar{\nu_\mu})$ denotes number of anti muon neutrinos reaching at detector as anti muon neutrinos and producing a μ^- lepton. In $\triangle R$, $(R_{4\nu})_{\delta c_{ij} \neq 0}$ denotes the ratio R in presence of CPT violating terms and $(R_{4\nu})_{\delta c_{ij}=0}$ denotes the ratio R in absence of CPT violating terms.

In presence of matter the observable R will not be equal to one, even if pure CPT violation is absent. It will be equal to a numerical value representing the ratio of neutrino and antineutrino interaction cross-sections. If we want to analyze the extent of deviation produced by pure CPT violation, we have to hide or filter out the deviation produced by any other phenomenon. In an attempt to filter out pure CPT violating contribution from the total observed deviation we take into record a new observable ΔR. This parameter is defined in the equation (45). Figs. 4 and 6 demonstrate the variation in R with energy whereas Figs. 5 and 7 exhibit the variation in ΔR with energy for baseline 7500 km. We observe that for a given long baseline, pure CPT violating effects get smaller with increase in energy. The presence of CPT violating signatures can be observed with neutrino factory and it can be checked by looking at R and ΔR plots (Fig. 4–Fig. 7) for different values of CPT violating parameter δc_{31}. As we know that in presence of sterile neutrino the manifestation of pure CPT signatures depends on the values of sterile parameters, hence the entire analysis is performed with two sets of best fit values of sterile parameters which were examined by different neutrino experiments. The observations from neutrino factory with sterile parameter values obtained from reactor+atmospheric experiments exhibit larger deviation in observables R and ΔR in comparison to the results obtained with sterile parameter values taken from long baseline experiments. These observables are checked for both mass hierarchies. From the Figs. 4, 5, 6 and 7 we comprehend that after 15 GeV there is a flip in sign of the observables for both the hierarchies. At the same time the amount of deviation measured for pure CPT violating effects are different for NH and IH for the same energy and baseline.

The next observable, asymmetry factor A_μ is defined as

$$A_\mu(E) \equiv \frac{N(\nu_\mu \to \nu_\mu)^{far}(E)}{N(\nu_\mu \to \nu_\mu)^{near}(E)} - \frac{N(\bar{\nu_\mu} \to \bar{\nu_\mu})^{far}(E)}{N(\bar{\nu_\mu} \to \bar{\nu_\mu})^{near}(E)} \tag{46}$$

This ratio is determined by using far and near detectors. The variations in asymmetry factor with energy for baseline 7500 km are shown by Figs. 8 and 9. These figures reflect the variations in observable A_μ for different values of δc_{31} (CPT violating parameter) and for both mass hierarchies. The $\delta c_{31} = 0$ will reflect A_μ values without any contribution from CPT violating terms.

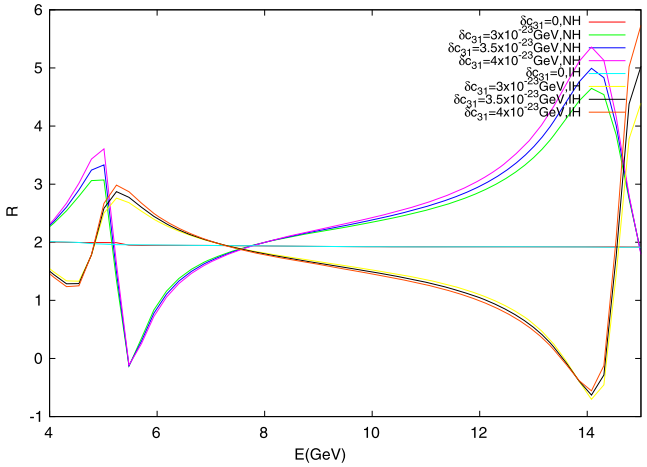

(a)

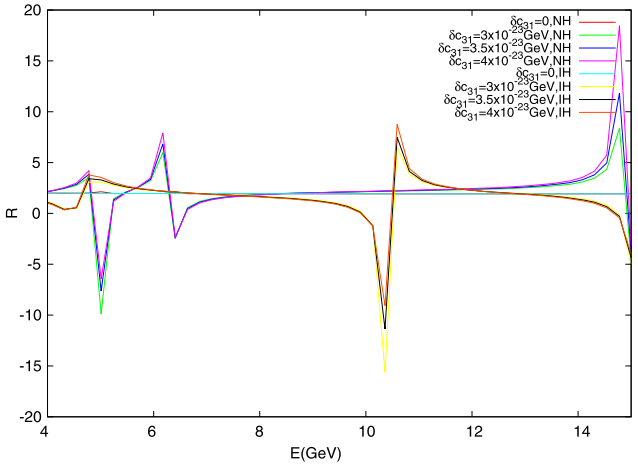

(b)

Fig. 4. The variation of R with energy in the energy range 4–15 GeV. Values of sterile parameters considered in plot (a) and plot (b) are selected from long baseline experiments and reactor+atm experiments respectively. These observations are made for different values of CPT violating parameter δc_{31}; (i) $\delta c_{31} = 0$ (setting CPT violating parameter to zero) (ii) $\delta c_{31} = 3 \times 10^{-23}$ GeV (iii) $\delta c_{31} = 3.5 \times 10^{-23}$ GeV (iv) $\delta c_{31} = 4 \times 10^{-23}$ GeV. For all the observations $\delta c_{21} = 3 \times 10^{-23}$ GeV.

The asymmetry factor increases with the increase in the value of δc_{31}. An enhancement in magnitude of asymmetry factor is also observed with the increase in values of sterile angles. Hence more stringent bounds on sterile parameters are required to check the extent of CPT violation.

In our work we have imposed bounds on CPT violating parameters δc_{31} and δc_{21} at 90% C.L. Figs. 10 and 11 demonstrate contours in δc_{31} and δc_{21} plane with true value of CPT violating parameters as $\delta c_{31} = 3 \times 10^{-23}$ GeV, $\delta c_{21} = 3 \times 10^{-23}$ GeV and $\delta c_{31} = 4 \times 10^{-23}$ GeV, $\delta c_{21} = 3 \times 10^{-23}$ GeV respectively. Each figure consists of three plots at three different energies 15 GeV, 25 GeV and 50 GeV for baseline 7500 km. These plots illustrate bounds on CPT violating parameters at mentioned energies. The selection of three different energies are based on the

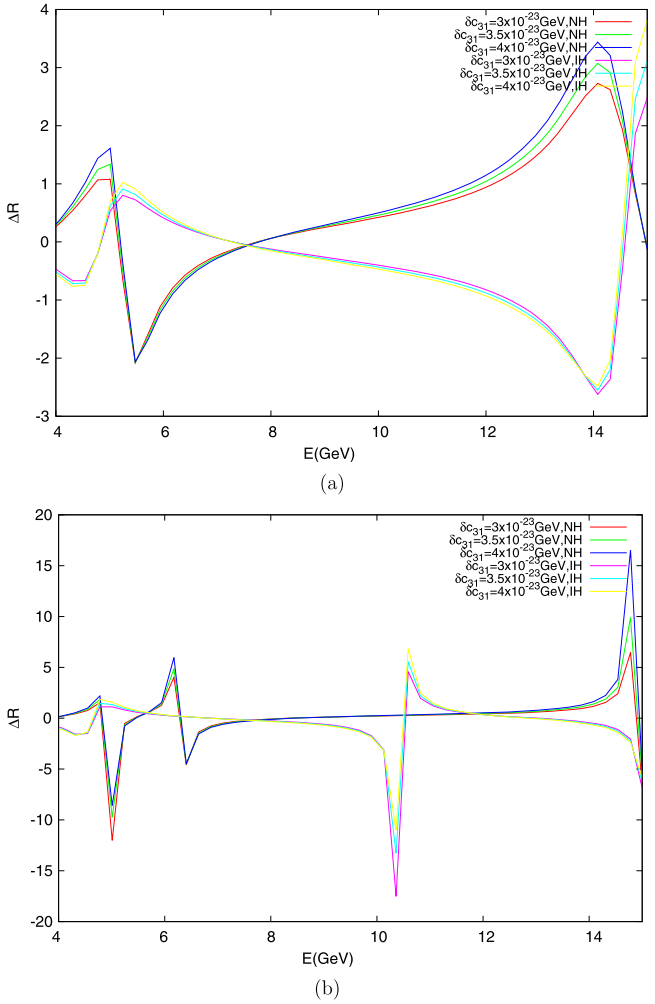

Fig. 5. The variation of $\triangle R$ with energy in the energy range 4–15 GeV. Values of sterile parameters considered in plot (a) and plot (b) are selected from long baseline experiments and reactor+atm experiments respectively. These observations are made for different values of CPT violating parameter δc_{31}; (i) $\delta c_{31} = 0$ (setting CPT violating parameter to zero) (ii) $\delta c_{31} = 3 \times 10^{-23}$ GeV (iii) $\delta c_{31} = 3.5 \times 10^{-23}$ GeV (iv) $\delta c_{31} = 4 \times 10^{-23}$ GeV. For all the observations $\delta c_{21} = 3 \times 10^{-23}$ GeV.

results of previous observations (i.e. R, ΔR and A_μ). At selected energy 15 GeV, change in sign (+ve to −ve) is observed in the observables while studying effects of CPT violation for considered baseline and energies. This observation makes 15 GeV energy important for studying CPT violating effects. A proposal of neutrino factory producing neutrino beam from 25 GeV muons is described in reference [69] whereas in a different proposal we have a 50 GeV muon beam for the production of neutrinos at neutrino factory [70]. Therefore, by checking at the extent of bounds imposed on CPT violating parameters with energies 25 GeV and 50 GeV we want to check that by what order the results will improve if we move towards higher energies. By looking at different energy contours we conclude that amongst the three selected energies, 50 GeV energy is

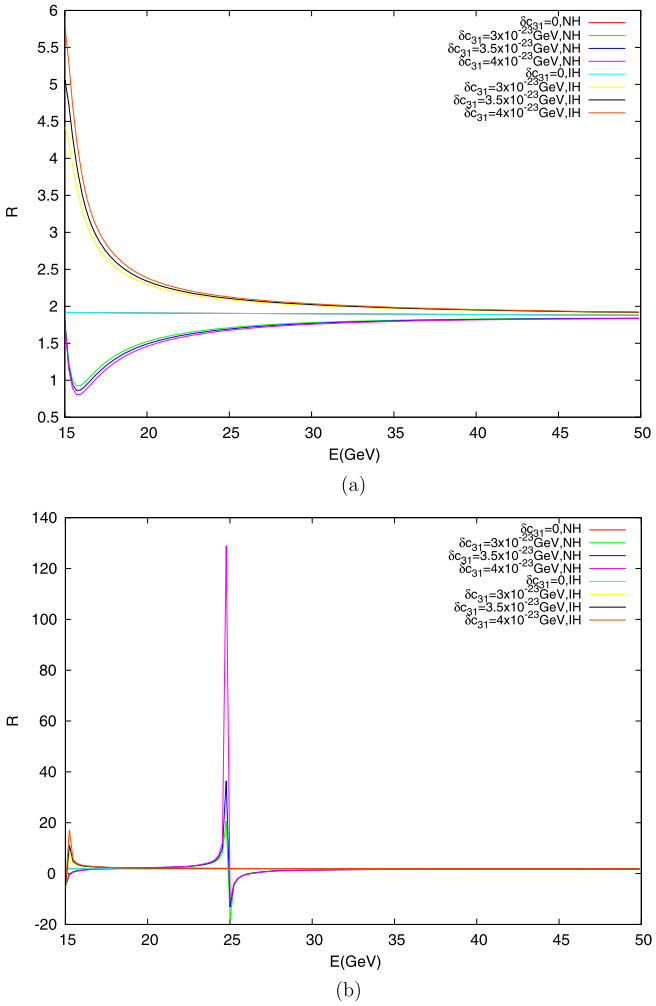

Fig. 6. The variation of R with energy in the energy range 15–50 GeV. Values of sterile parameters considered in plot (a) and plot (b) are selected from long baseline experiments and reactor+atm experiments respectively. These observations are made for different values of CPT violating parameter δc_{31} (i) $\delta c_{31} = 0$ (setting CPT violating parameter to zero) (ii) $\delta c_{31} = 3 \times 10^{-23}$ GeV (iii) $\delta c_{31} = 3.5 \times 10^{-23}$ GeV (iv) $\delta c_{31} = 4 \times 10^{-23}$ GeV. For all the observations $\delta c_{21} = 3 \times 10^{-23}$ GeV.

the best suited energy to constrain CPT violating parameter δc_{31}, if nature allows NH to be the true hierarchy. At the same time we observe that for long baseline experiments with energies less than 15 GeV, IH will be a favorable hierarchy for the determination of bounds on CPT violating parameters.

As discussed earlier that, out of two parameters δc_{31} and δc_{21} considered in our analysis, the variation in δc_{31} will produce larger variation in the detectable observables which are used in our work for checking CPT violation. Fig. 12 shows value of χ^2 as a function of CPT violating parameter δc_{31}. It is plotted by marginalizing over oscillation parameters Δm^2_{31} in 3σ range of their best fit values and δ_{CP} in 0 to 2π range. Looking at figure we observe that neutrino factory

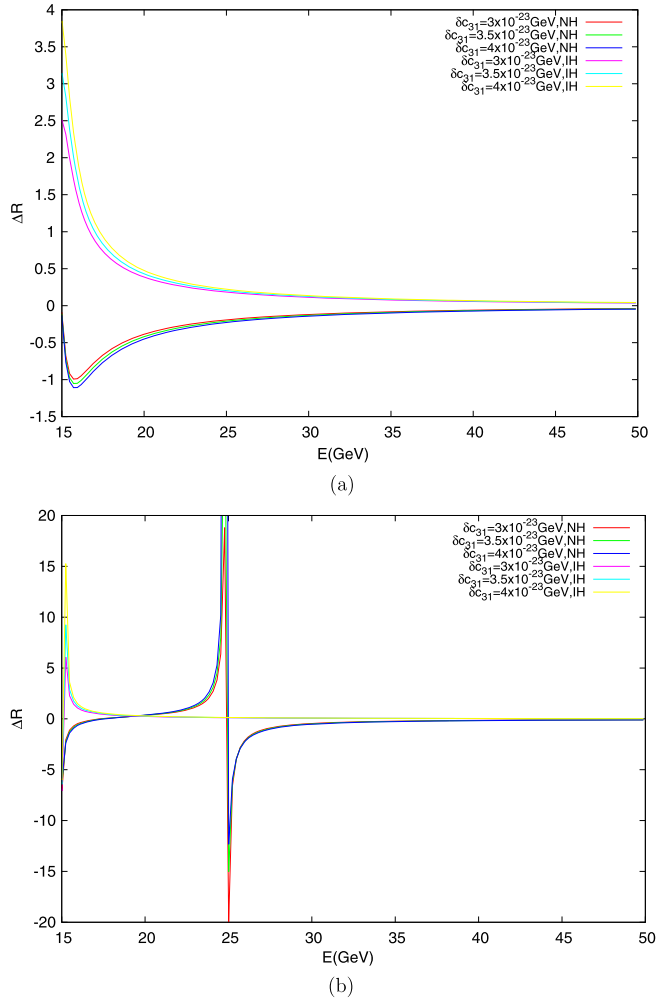

Fig. 7. The variation of $\triangle R$ with energy in the energy range 15–50 GeV. Values of sterile parameters considered in plot (a) and plot (b) are selected from long baseline experiments and reactor+atm experiments respectively. These observations are made for different values of CPT violating parameter δc_{31} (i) $\delta c_{31} = 0$ (setting CPT violating parameter to zero) (ii) $\delta c_{31} = 3 \times 10^{-23}$ GeV (iii) $\delta c_{31} = 3.5 \times 10^{-23}$ GeV (iv) $\delta c_{31} = 4 \times 10^{-23}$ GeV. For all the observations $\delta c_{21} = 3 \times 10^{-23}$ GeV.

with an exposure time of 500 Kt-yr will be capable of capturing CPT violating signatures when CPT violating parameter $\delta c_{31} \geqslant 3.6 \times 10^{-23}$ GeV for NH and $\delta c_{31} \geqslant 4 \times 10^{-23}$ GeV for IH at 3σ level.

5. Conclusions

Neutrino factory will provide us a potential setup for observing T violation and setting significant bounds on CPT violation in neutrino sector. In four $(3 + 1)$ neutrino flavor framework the angular mixing parameters of three active neutrinos are well constrained while the sterile parameters still need better bounds on them. With the change in the value of sterile parameters

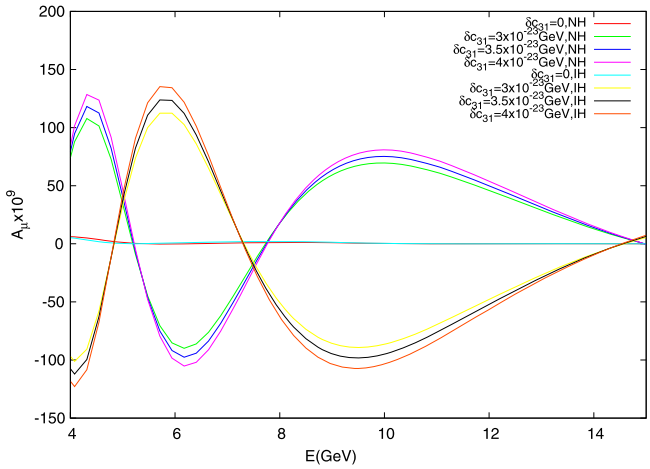

(a)

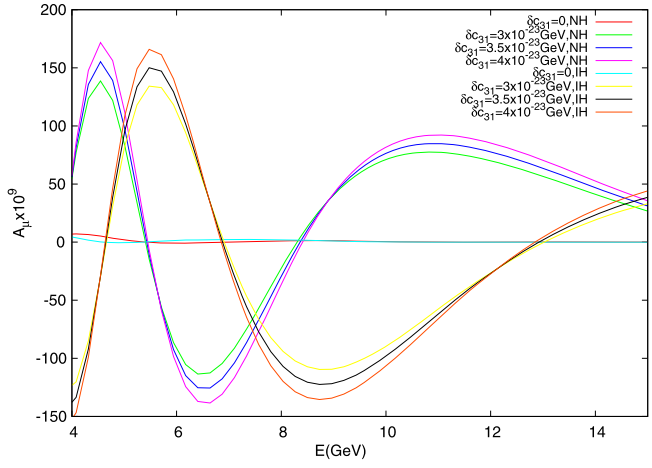

(b)

Fig. 8. The variation in asymmetry factor A_μ(E) as a function of energy in energy range 4–15 GeV. Values of sterile parameters considered in plot (a) and plot (b) are taken from long baseline experiments and reactor+atm experiments respectively.

a notable variation in bounds on CPT violating parameter and on the extent of T violation is captured by neutrino factory. Hence, well constrained values of sterile parameters will allow any neutrino experiment to impose better constraints on T violation and CPT violating parameters. Amongst two selected sets of values of sterile parameters i.e. from long baseline experiments and from reactor+atmospheric experiments we observed that the potential of neutrino factory for investigating T and CPT violation enhances when the sterile parameters values are equal to those which are constrained by reactor and atmospheric experiments. Neutrino factory with 50 GeV energy will be sensitive to probe T violation through $\nu_\mu \to \nu_\tau$ channel if true values of sterile parameters are equal to those predicted by reactor+atmospheric experiments. We stipulate that a pure CPT violating effects can be observed along short baseline i.e. 1300 km–2000 km with energies 4 GeV to 6 GeV, where extrinsic CPT violation is negligible. On the other hand

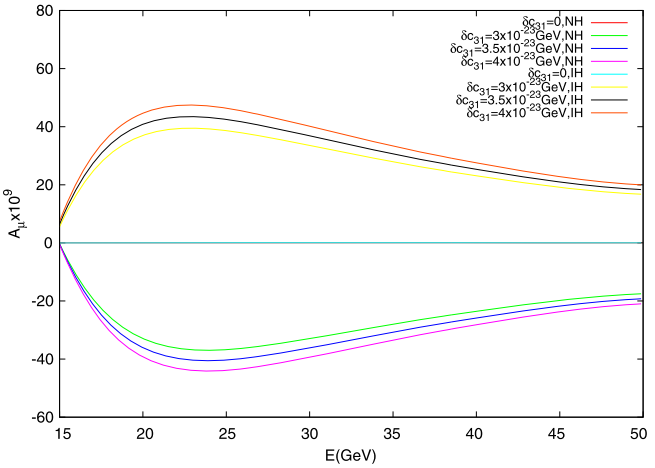

(a)

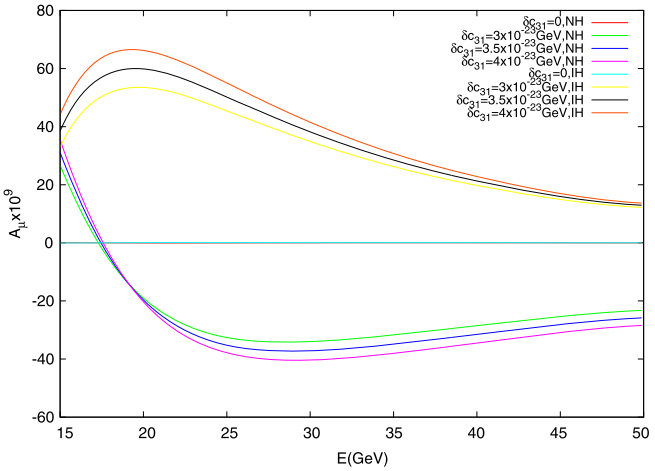

(b)

Fig. 9. The variation in asymmetry factor A_μ(E) as a function of energy in energy range 15–50 GeV. Values of sterile parameters considered in plot (a) and plot (b) are taken from long baseline experiments and reactor+atm experiments respectively.

at long baselines we can observe these effects with energies in the range 14 GeV–40 GeV along baselines 4000 km–7500 km. CPT violating parameter $\delta c_{31} \geqslant 3.6 \times 10^{-23}$ GeV for NH and $\delta c_{31} \geqslant 4 \times 10^{-23}$ GeV for IH will make neutrino factory capable to capture signatures of CPT violation at 3σ level.

Acknowledgements

One of the authors Sujata Diwakar is thankful to University Grant Commission, India (F1-17.1/2011-12/RGNF-SC-UTT-3413/SA-III/website) for giving financial support under the Rajiv Gandhi National Fellowship scheme.

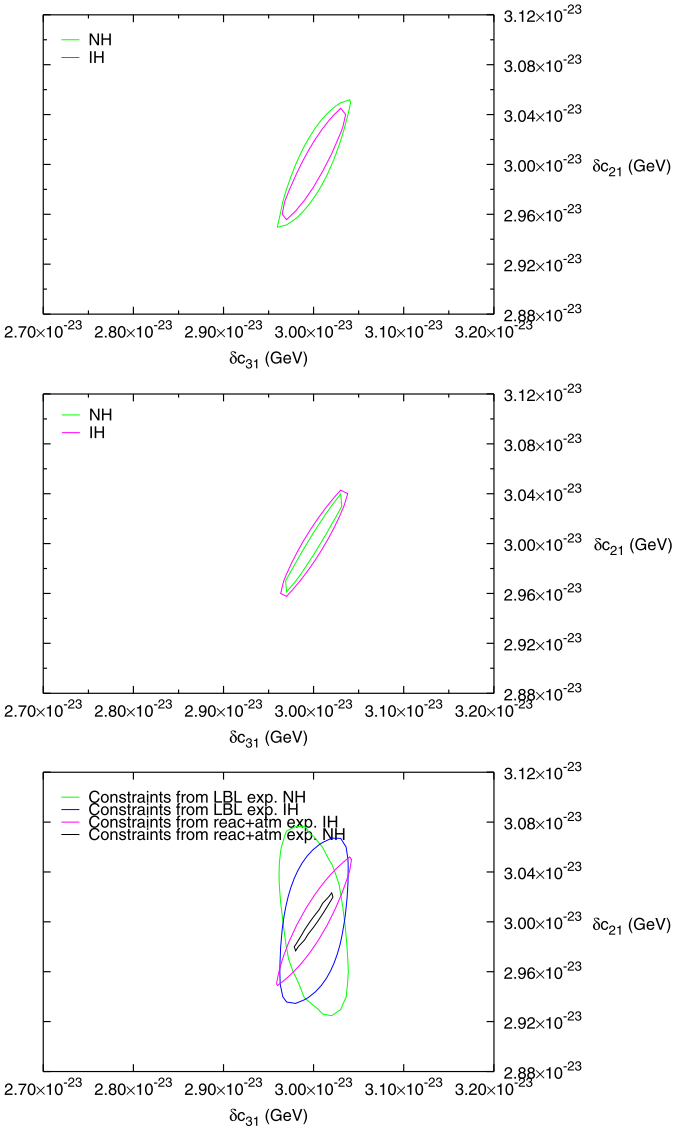

Fig. 10. The contours are plotted in δc_{31}–δc_{21} plane for 90% C.L. with CPT violating terms $\delta c_{31} = \delta c_{21} = 3.0 \times 10^{-23}$ GeV taking energies 15 GeV, 25 GeV and 50 GeV respectively. In top two plots sterile parameters values are taken from reactor+atmospheric experiments while for the bottom plot these values are taken from both the reactor+atmospheric and long baseline experiments.

Appendix A. Eigenvalues and eigenvectors of hamiltonian to second order

Using the time independent perturbation theory we calculate the eigenvalues and eigenvectors of hamiltonian H_f up to the order of η^2 correctly.

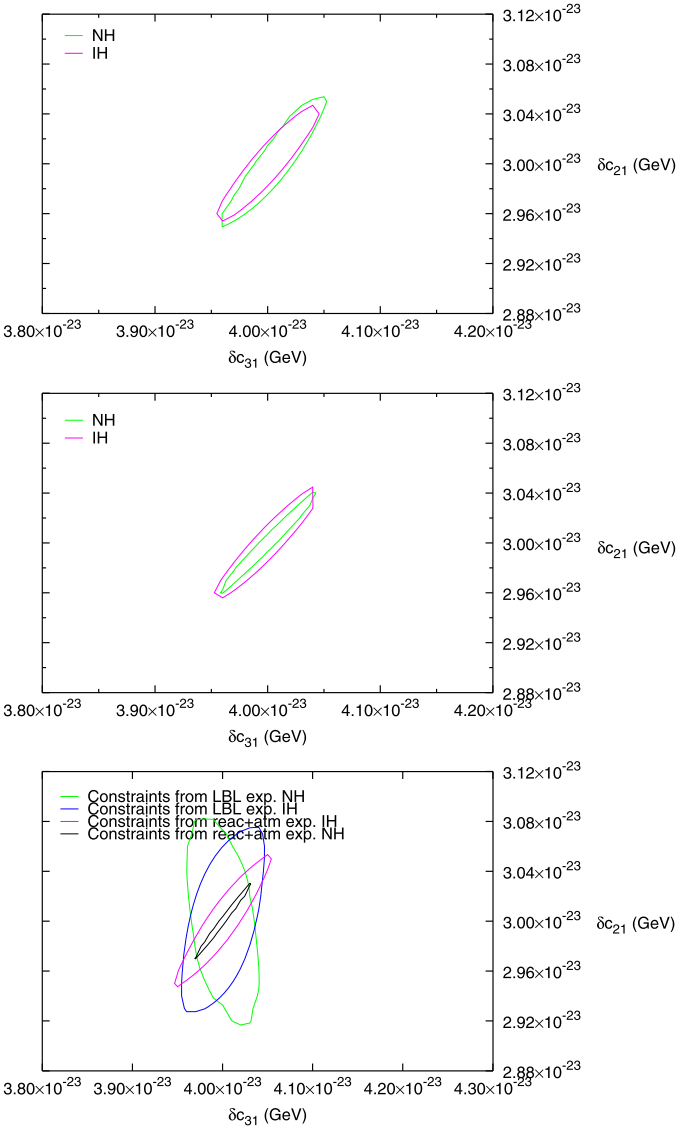

Fig. 11. The contours are plotted in δc_{31}–δc_{21} plane for 90% C.L. with CPT violating terms $\delta c_{31} = 4.0 \times 10^{-23}$ and $\delta c_{21} = 3.0 \times 10^{-23}$ GeV taking energies 15 GeV, 25 GeV and 50 GeV respectively. In top two plots sterile parameters values are taken from reactor+atmospheric experiments while for the bottom plot these values are taken from both the reactor+atmospheric and long baseline experiments.

Eigenvalues of H_0 are given by

$$E_1^{(0)} = a_e + a_n,\ E_2^0 = a_n,\ E_3^{(0)} = a_e + 1,\ E_4^{(0)} = \sigma \tag{A.1}$$

where $\sigma = \dfrac{\triangle m_{41}^2}{\triangle m_{31}^2}$ and $a_{e,n} \equiv \dfrac{A_{e,n}}{\triangle m_{31}^2}$.

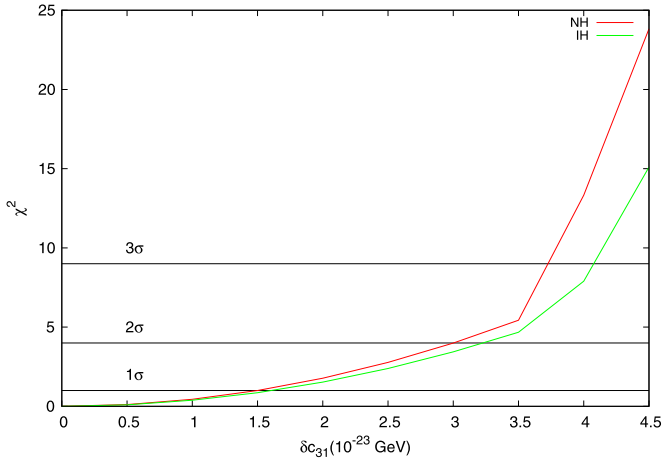

Fig. 12. χ^2 as a function of δc_{31} is shown. The green curve represents inverted hierarchy and red curve represents normal hierarchy as true hierarchy.

Eigenvectors of H_0 are given by

$$V_1^{(0)} = \begin{bmatrix} 1 \\ 0 \\ 0 \\ 0 \end{bmatrix}, V_2^{(0)} = \begin{bmatrix} 0 \\ -c_{23} \\ s_{23} \\ 0 \end{bmatrix}, V_3^{(0)} = \begin{bmatrix} 0 \\ s_{23} \\ c_{23} \\ 0 \end{bmatrix}, V_4^{(0)} = \begin{bmatrix} 0 \\ 0 \\ 0 \\ 1 \end{bmatrix} \tag{A.2}$$

Eigenvalues and eigenvectors for H_1 are calculated by using equations (A.3) and (A.4) respectively.

$$E_j^{(1)} = < V_j^0 \mid H_1 \mid V_j^0 > \tag{A.3}$$

$$\mid V_j^{(1)} >= \sum_{k \neq j} \mid V_k^0 > \frac{< V_j^0 \mid H_1 \mid V_j^0 >}{E_j^{(0)} - E_k^{(0)}} \tag{A.4}$$

Eigenvalues and eigenvectors of H_2 can be calculated with the help of zeroth and first order eigenvalues and eigenvectors mentioned in equations (A.5) and (A.6) given as

$$E_j^{(2)} = < V_j^0 \mid H_1 \mid V_j^1 > \tag{A.5}$$

$$\mid V_j^{(2)} >= \frac{- \mid V_j^{(0)} >}{2} \sum_{k \neq j} \frac{\mid V_{jk} \mid^2}{E_{kj}^2} + \sum_{k \neq j} \mid V_k^{(0)} > \left[\sum_{k' \neq j} \frac{V_{kj'} V_{k'j}}{E_{kj} E_{k'j}} - \frac{V_{kj} V_{jj}}{E_{kj}^2} \right] \tag{A.6}$$

where

$$V_{kj} = < k^0 \mid V \mid j^0 > \text{ and } E_{kj} = E_k^0 - E_j^0$$

The total eigenvalues and eigenvectors of H_f up to second order are given by

$$E_{total} = E_j^0 + E_j^1 + E_j^2 \tag{A.7}$$

$$V_{total} = V_j^0 + V_j^1 + V_j^2 \tag{A.8}$$

Using the set of four normalized eigenvectors we form the unitary matrix $\tilde{U}$ as.

$$\tilde{U} = \begin{bmatrix} (V_{1m})_1 & (V_{1m})_2 & (V_{1m})_3 & (V_{1m})_4 \\ (V_{2m})_1 & (V_{2m})_2 & (V_{2m})_3 & (V_{2m})_4 \\ (V_{3m})_1 & (V_{3m})_2 & (V_{3m})_3 & (V_{3m})_4 \\ (V_{4m})_1 & (V_{4m})_2 & (V_{4m})_3 & (V_{4m})_4 \end{bmatrix} \tag{A.9}$$

where V_{jm} is normalized vector.

Now hamiltonian H_f can be diagonalized by using the above derived unitary matrix $\tilde{U}$ and the diagonalized hamiltonian H_D can be expressed as

$$H_D = \tilde{U}^\dagger H_f \tilde{U} \tag{A.10}$$

References

[1] Q.R. Ahmad, et al., SNO Collaboration, Phys. Rev. Lett. 89 (2002) 011302.
[2] S.N. Ahmed, et al., SNO Collaboration, Phys. Rev. Lett. 92 (2004) 181301, arXiv:nucl-ex/0309004.
[3] K. Eguchi, et al., KamLAND Collaboration, Phys. Rev. Lett. 90 (2003) 021802.
[4] C. Athanassopoulos, et al., LSND collaboration, Phys. Rev. Lett. 77 (1996) 3082, arXiv:nucl-ex/9605003.
[5] C. Athanassopoulos, et al., LSND collaboration, Phys. Rev. Lett. 75 (1995) 2650.
[6] C. Athanassopoulos, et al., LSND collaboration, Phys. Rev. Lett. 81 (1998) 1774, arXiv:nucl-ex/9709006.
[7] C. Athanassopoulos, et al., LSND collaboration, Phys. Rev. C 58 (1998) 2489, arXiv:nucl-ex/9706006.
[8] A. Aguilar, et al., LSND Collaboration, Phys. Rev. D 64 (2001) 112007, arXiv:hep-ex/0104049.
[9] C. Athanassopoulos, et al., LSND collaboration, Phys. Rev. Lett. 77 (1996) 3082, arXiv:nucl-ex/9605003.
[10] MiniBooNE, A.A. Aguilar-Arevalo, et al., Phys. Rev. Lett. 105 (2010) 181801, arXiv:1007.1150.
[11] Janet M. Conrad, arXiv:1306.6494v1 [hep-ex].
[12] W.M. Yao, et al., Particle data group, J. Phys. G 33 (2006) 1.
[13] K. Nakamura, et al., Particle data group, J. Phys. G 37 (2010) 075021 [SPIRES].
[14] B.A. Reid, L. Verde, R. Jimenez, O. Mena, J. Cosmol. Astropart. Phys. 1001 (2010) 003, arXiv:0910.0008 [hep-ph].
[15] M.C. Gonzalez-Garcia, M. Maltoni, J. Salvado, J. High Energy Phys. 1008 (2010) 117, arXiv:1006.3795 [hep-ph].
[16] J. Hamann, S. Hannestad, G.G. Raffelt, I. Tamborra, Yvonne Y.Y. Wong, Phys. Rev. Lett. 105 (2010) 181301, arXiv:1006.5276 [astro-ph].
[17] E. Giusarma, M. Corsi, M. Archidiacono, R. de Putter, A. Melchiorri, O. Mena, S. Pandolfi, Phys. Rev. D 83 (2011) 115023, arXiv:1102.4774 [astro-ph].
[18] Z. Hou, R. Keisler, L. Knox, M. Millea, C. Reichardt, arXiv:1104.2333 [astro-ph].
[19] Y.I. Izotov, T.X. Thuan, Astrophys. J. 710 (2010) L67, arXiv:1001.4440 [astro-ph].
[20] E. Aver, K.A. Olive, E.D. Skillman, J. Cosmol. Astropart. Phys. 1005 (2010) 003, arXiv:1001.5218 [astro-ph].
[21] Jing-Fei Zhang, Yun-He Li, Xin Zhang, arXiv:1408.4603v2 [astro-ph].
[22] F. Beutler, C. Blake, M. Colless, D.H. Jones, et al., Mon. Not. R. Astron. Soc. 416 (2011) 3017, arXiv:1106.3366 [astro-ph].
[23] C. Blake, S. Brough, M. Colless, C. Contreras, et al., Mon. Not. R. Astron. Soc. 425 (2012) 405, arXiv:1204.3674 [astro-ph].
[24] N. Padmanabhan, X. Xu, D.J. Eisenstein, R. Scalzo, et al., Mon. Not. R. Astron. Soc. 427 (2012) 2132, arXiv:1202.0090 [astro-ph].
[25] L. Anderson, E. Aubourg, S. Bailey, D. Bizyaev, et al., Mon. Not. R. Astron. Soc. 427 (2012) 3435, arXiv:1203.6594 [astro-ph].
[26] C.L. Bennett, D. Larson, J.L. Weiland, N. Jarosik, et al., arXiv e-prints, arXiv:1212.5225 [astro-ph], 2012.
[27] F. Kaether, W. Hampel, G. Heusser, J. Kiko, T. Kirsten, Phys. Lett. B 685 (2010) 47–54, arXiv:1001.2731 [math.AG].
[28] J.N. Abdurashitov, et al., SAGE Collaboration, Phys. Rev. C 80 (2009) 015807, arXiv:0901.2200 [nucl-ex].
[29] C. Guinti, et al., arXiv:1210.5715 [hep-ph].
[30] C. Guinti, http://dx.doi.org/10.5506/APhysPolBSupp.6.667.
[31] V. Barger, Y. Gao, D. Marfatia, arXiv:1109.6748v2 [hep-ph], 2011.
[32] P. Adamson, et al., MINOS Collaboration, Phys. Rev. Lett. 107 (2011) 011802, arXiv:1104.3922 [hep-ex].
[33] D. Hernandez, A.Y. Smirnov, Phys. Lett. B 706 (2012) 360, arXiv:1105.5946 [hep-ph].
[34] C. Giunti, M. Laveder, arXiv:1109.4033 [hep-ph].
[35] I.E. Stockdale, et al., Phys. Rev. Lett. 52 (1984) 1384.

[36] D.O. Caldwell, R.N. Mohapatra, Phys. Rev. D 48 (1993) 3259.
[37] S. Geer, Phys. Rev. D 57 (1998) 6989;
S. Geer, Phys. Rev. D 59 (1999) 039903 [Erratum], arXiv:hep-ph/9712290.
[38] A. De Rujula, M.B. Gavela, P. Hernandez, Nucl. Phys. B 547 (1999) 21.
[39] C. Albright, G. Anderson, V. Barger, et al., arXiv:hep-ex/0008064.
[40] A. Blondel, et al., Nucl. Instrum. Methods A 467 (2000) 102.
[41] M. Apollonio, et al., CERN working group on oscillation physics at Neutrino Factory, arXiv:hep-ph/0210192, 2002.
[42] A. Bandyopadhyay, et al., ISS Physics working group, Rep. Prog. Phys. 72 (2009) 106201, arXiv:0710.4947 [hep-ph].
[43] Animesh Chatterjee, Raj Gandhi, Jyotsna Singh, arXiv:1402.6265v1 [hep-ph], 2014.
[44] Osamu Yasuda, arXiv:1004.2388v1.
[45] FERMILAB-CONF-13-300.
[46] Stephen J. Parke, Thomas J. Weiler, Phys. Lett. B 501 (2001) 106, arXiv:hep-ph/0011247v2.
[47] Davide Meloni, Jian Tang, Walter Winter, Phys. Rev. D 82 (2009) 093008, arXiv:1007.2419v2 [hep-ph].
[48] Arman Esmaili, Francis Halzen, O.L.G. Peres, J. Cosmol. Astropart. Phys. B 07 (2013) 048, arXiv:1303.3294v2 [hep-ph].
[49] A. Donini, M. Maltoni, D. Meloni, P. Migliozzi, F. Terranova, J. High Energy Phys. 0712 (013) (2007), arXiv:0704.0388 [hep-ph].
[50] International Design study of the neutrino factory, http://www.ids-nf.org.
[51] P. Huber, M. Lindner, M. Rolinec, W. Winter, Phys. Rev. D 74 (2006) 073003, arXiv:hep-ph/0606119.
[52] P. Huber, M. Lindner, W. Winter, Nucl. Phys. B 6453 (2002), arXiv:hep-ph/0204352.
[53] E. Ables, et al., MINOS, FERMILAB-PROPOSAL-P-875.
[54] C.H. Albright, et al., Neutrino Factory/Muon Collider Collaboration, arXiv:Physics/0411123.
[55] Jian Tang, Walter Winter, Phys. Rev. D 80 (2009) 053001, arXiv:0903.3039v2.
[56] R.J. Geller, T. Hara, Nucl. Instrum. Methods A 503 (2003) 187, arXiv:hep-ph/0111342.
[57] T. Ohlsson, W. Winter, Phys. Rev. D 68 (2003) 073007, arXiv:hep-ph/0307178.
[58] P. Huber, M. Lindner, W. Winter, Comput. Phys. Commun. 167 (2005) 195, http://www.mpi-hd.mpg.de/Lin/globes/; arXiv:hep-ph/0407333.
[59] P. Huber, J. Kopp, M. Lindner, M. Rolinec, W. Winter, Comput. Phys. Commun. 177 (2007) 432, arXiv:hep-ph/0707118.
[60] M.C. Gonzalez-Garcia, M. Maltoni, T. Schwetz, arXiv:1512.06856v1 [hep-ph].
[61] Anindya Datta, Raj Gandhi, Poonam Mehta, S. Uma Sankar, Phys. Lett. B 597 (2004) 356, arXiv:hep-ph/0312027v2.
[62] J.N. Bahcall, V. Barger, D. Marfatia, Phys. Lett. B 534 (2002) 120, arXiv:hep-ph/0201211.
[63] V.D. Barger, S. Pakvasa, T.J. Weiler, K. Whisnant, Phys. Rev. Lett. 85 (2000) 5055, arXiv:hep-ph/0005197.
[64] A. Dighe, S. Ray, Phys. Rev. D 78 (2008) 036002, arXiv:0802.0121 [hep-ph].
[65] A. Samanta, Phys. Lett. B 693 (2010) 296, arXiv:1005.4851 [hep-ph].
[66] M.C. Gonzalez-Garcia, M. Maltoni, Phys. Rev. D 70 (2004) 033010, arXiv:hep-ph/0404085.
[67] Magnus Jacobson, Tommy Ohlsson, Phys. Rev. D 69, 013003, arXiv:hep-ph/0305064v3.
[68] Sujata Diwakar, Jyotsna Singh, Yogita Pant, R.B. Singh, Extrinsic CPT violation with sterile neutrino, Int. J. Res. Eng. Technol. 05 (04) (2016) 66–72, esatjournals.net/ijret/2016v05/i05/IJRET20160505014.pdf.
[69] Study of Low-energy Neutrino factory at the Fermilab to DUSEL Baseline, inspirehep.net/record/829747/files/fermilab-fn-0836-apc.pdf.
[70] The study of a European Neutrino Factory complex, CERN/PS/2002-080(PP).